

Chapter 2

Light-Tracking Kinematics of Mobile Platform

Ahmad Salahuddin Mohd Harithuddin, Pavel M. Trivailo,
and Reza N. Jazar

Abstract The formulation of tracking mechanism used for a light-tracking system is presented to maximize the collected energy. The solution considers the motion of the illumination sources and the translational and rotational motion of the light-receiver/collector. The tracker in consideration consists of two orthogonal rotary actuators to provide a hemispherical pointing capability. The tracker is assumed to be mounted on a mobile platform, such as a rover or a robot, which moves on a given path. The tracker's function is to change the orientation of the light-collector to face and receive the maximum incident radiation from multiple light sources. As the platform carrying the tracker is moving, the lights' positions and intensity may vary. This requires the tracker to actively point its payload towards the orientation that receives maximum light intensity while being in motion. An example of an indoor robot tracking radiant energy from fluorescent lights in a room is presented to demonstrate the concept. In addition, the coordinate transformation method using compound homogeneous transformation matrix is applied in the formula derivation.

2.1 Introduction

The function of a tracking system is to follow the motion of a relatively moving object, such as a light source, for purposes such as surveillance and energy reception. The current treatment of light tracking system usually deals with a single target of interest—tracking the Sun's motion for solar energy harvesting purposes.

A.S.M. Harithuddin • P.M. Trivailo • R.N. Jazar (✉)
School of Aerospace, Mechanical and Manufacturing Engineering, RMIT University, Melbourne,
VIC, Australia
e-mail: s3305201@student.rmit.edu.au; pavel.jazar@rmit.edu.au; reza.jazar@rmit.edu.au

The equation of motion of the Sun is usually given in ecliptic coordinates [1]. Hence, it is necessary to perform a set of coordinate transformations to program an Earth-based Sun-tracker to trace its motion. A more complicated example is a mobile robot exposed to multiple light sources.

An example of a setting with multiple light sources can be found in an indoor environment where radiance is provided by a combination of artificial and non-artificial lights (for example, radiance from fluorescent lamps and window lighting). The present photovoltaic panels are not optimized for extracting electrical power from indoor radiation into direct current electricity; however, works by Randall [10] and Sansoni et al. [12] show promises in the development of specialized photovoltaic cells to be used in Sunless settings. Another interesting multiply-lighted environment is a mobile robots in the polar regions. A solar-powered robot, aptly named Cool Robot [8], is used to conduct scientific experiments in the extreme climate of the South Pole. Exploiting the snowy environment, the solar panels are designed to generate photovoltaic energy from both the Sun and its snow-reflected component.

This article approaches the tracking system as a motion kinematics concept with a focus on the formula used by tracker to follow the target motion. The source can be from a single or multiple light sources. The tracker is assumed to be working without any help from a photosensor, i.e. the tracker follows a precalculated translation and orientation trajectory in order to receive maximum light intensity. In this article, the derivation of such formula is presented for the application of a ground-fixed solar tracker and a photovoltaic panels on a rover.

The existing methods for switching coordinates between reference frames use either spherical trigonometric technique or rotation matrix. In this article, the coordinate transformation includes both rotation and translation, using the 4×4 homogeneous transformation matrix.

To demonstrate the application of the analytical result, the problem of an illumination tracking photovoltaic panel on a moving platform, under multiple radiant energy sources is presented. The objective of the two-degree-of-freedom, dual-axis tracker is to assure that the maximum possible radiant energy intensity from multiple sources reaches the surface of the photovoltaic panels. To determine the angular trajectories, i.e. the azimuth and elevation angles of the panel, and the power usage of the system, the path of the vehicle and the illumination placements around the environment must be known a priori. The trajectories are determined such that the panel is oriented towards the direction which receives the most light intensity. The method for the maximization of electricity production for an indoor photovoltaic system in artificially lighted environment proposed in those paper is, at least to the knowledge of the authors, a novelty in the field of the light tracking system.

2.2 Previous Work

Formula-based, light-tracking method receives considerable attention especially in solar energy research as solar panels with tracking capabilities are more efficient than fixed-panels in harvesting energy from the radiant source. Traditionally, the equations for the apparent motion of the Sun and the intensity of the Sunray on an angled surface are described using spherical trigonometry which is mainly based on the work of astrodynamics [1]. Dealing with trigonometric calculation in technical computing tools, however, is not as straightforward as compared to working with matrix and vector operations. The vectorial approach, hence, has got more attention from researchers and practitioners in describing tracking formulas [9, 11, 13].

The next development to achieve a general Sun-tracking formula is done by Chen in conjunction with thermal solar energy [2]. They developed a tracking formula for a heliostat to direct and focus Sunlight onto a fixed target on the Earth. The formula is developed specifically for a rotation-elevation tracker. In 2006, Chen et al. derived a more versatile formula that also is applicable for heliostat with any type of orientation axes [3]. The formula can be used for an arbitrary located target.

Chong and Wong [4] derived a more general formula for the case of solar panels. Unlike the reflector, the solar panel is required to align its normal axis parallel to the Sun vector in order to receive maximum radiant energy. The formula is suitable for the application of azimuth-elevation and tip-tilt trackers.

These developments, however, only deal with tracker a single object, i.e. the Sun. The trackers in consideration of the authors also are assumed to be fixed on the Earth-surface frame. This work presents an improvement to the versatility of the existing formulas by generalizing the light tracking formula for any radiant energy-harvesting mechanism, including artificial lights in indoor settings. This includes the consideration of tracking multiple light sources and tracking on a moving platform for application in rovers and mobile robots. This work also focuses on the application of compound homogeneous transformation matrix in the problem of tracking radiant energy.

The type of radiance collector in this study can exist in the form of solar cells and indoor photovoltaic cells, which application requires the collector to be orientated towards a light source. For intermediate light receiver application, such as parabolic reflector or concentrator, the ray-tracing formula presented here can be further modified to include reflected light analysis.

2.3 Types of Tracker

Trackers can be grouped into classes by the number of the rotational degree-of-freedom: single axis trackers and dual axes trackers. Both types of trackers can be grouped in several subclasses by the orientation of the axes.

Fig. 2.1 Horizontal axis tracker

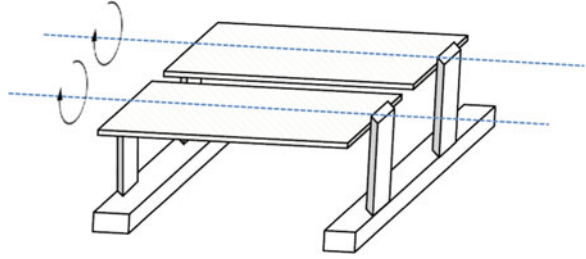


Fig. 2.2 Vertical axis tracker

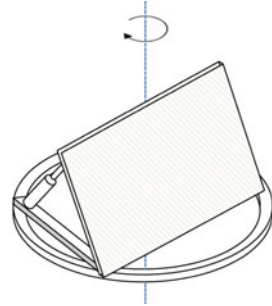
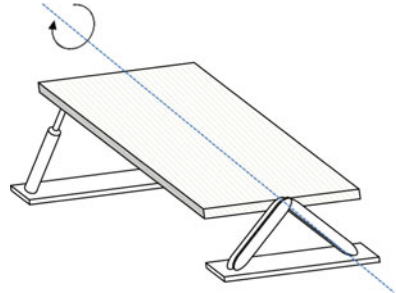


Fig. 2.3 Tilt axis tracker



2.3.1 Single Axis

Figure 2.1 shows a *horizontal axis tracker's* structure with a long, rotatable horizontal tube which is supported on bearing mounted on a frame structure. The photovoltaic module is installed on the horizontal tube facing upward to track the elevation of the Sun. A *vertical axis tracker* in Fig. 2.2 has an axis of rotation that is vertical to the ground with slanted photovoltaic modules that changes orientation from east to west to follow the azimuthal motion of the Sun. A *tilted axis tracker* shown in Fig. 2.3 has a similar setup to its horizontal counterpart with the tube slightly tilted several degrees from the ground.

Fig. 2.4 Tilt-roll dual axis tracker

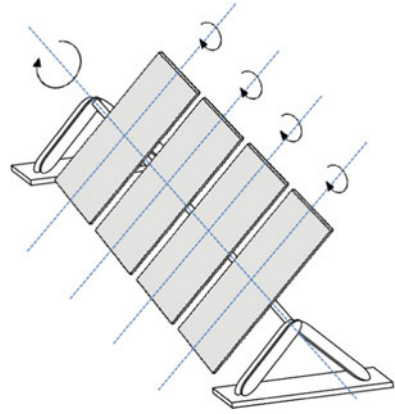
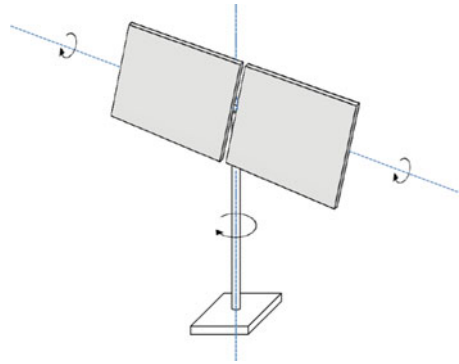


Fig. 2.5 Azimuth-elevation dual axis tracker



2.3.2 Dual Axes

Tilt-roll and *azimuth-elevation* are the two most commonly used dual axis configurations in solar tracking system. These trackers are free to rotate about two orthogonal axes, giving full orientation flexibility in tracking the Sun. The tilt-roll tracker has a configuration where its primary axis of rotation is parallel to the ground and its secondary axis is orthogonal to the primary axis as shown in Fig. 2.4. The azimuth-elevation tracker rotates about the azimuth axis, which is parallel to the zenith axis, as its primary axis and then rotates about the elevation axis, which is parallel to the ground as shown in Fig. 2.5. With two rotational degree-of-freedom, a dual axes tracker can track the Sun's azimuth and elevation angles throughout daytime.

2.4 Illuminance and Light Vectors

To assess the problem quantitatively, the illumination characteristics in the environment must be calculated before any information can be provided to the tracking control system. The direction of the brightest illumination with respect to vehicle's

position and orientation in the room must be predetermined. Radiant energy sources for photovoltaic cells can be obtained from the Sun (one single source), its reflected component (e.g., heliostats, snow), fluorescent tube lights, or window lighting.

2.4.1 Illuminance Computation

The illuminance received by a photovoltaic cells depends on the distance between the radiant energy source emitter and the receiver. Generally, the illuminance, E_s , is inversely proportional to the square of the distance of the source [10],

$$E_r = \frac{I}{r^2} \quad (2.1)$$

where I is the light intensity and r is the distance of the receiver from the light source. The illuminance E_r can also be measured as a function of the angle of incidence between the panel surface and the light direction [10],

$$E_\varphi = I \cos \varphi \quad (2.2)$$

where φ is the angle of incidence.

In the case of solar illuminance, the distance is not a factor; hence, Eq. (2.2) is sufficient. For a more general case, we will assume that the irradiance received from a light source is affected both by the distance between the emitter and the receiver and the angle of incidence of the incoming light ray:

$$E = \frac{I}{r^2} \cos \varphi. \quad (2.3)$$

In case of multiple light sources, we need to calculate the resultant of the amount of the illuminance of light rays from multiple emitters at the photovoltaic panel as shown in Fig. 2.6. Assuming that there are n emitters and the intensity of each source is I_i , we combine illuminance from multiple sources by a linear combination. The unit normal vector of the photovoltaic plane, $\hat{\mathbf{n}}$, is used to define the pointing direction of the panel and the unit vector, $\hat{\mathbf{r}}_i$, represents the light direction from the i th source as seen from the receiver:

$$E = \sum_i^n \frac{I_i}{r_i^2} \cos \varphi_i = \sum_i^n \frac{I_i}{r_i^2} \hat{\mathbf{n}} \cdot \hat{\mathbf{r}}_i \quad (2.4)$$

The objective of an automated tracker is to find the pointing direction such that the photovoltaic panel receives the maximum possible radiant energy from the multiple sources, that is, to find a vector $\hat{\mathbf{n}}$ such that E in Eq. (2.4) is maximum. Such vector $\hat{\mathbf{n}}$ is defined as *maximum illuminance vector*. Note that, in this work, Eq. (2.4) does not give the actual illuminance in photometry sense but is used to provide a method to quantify the illuminance based on the distances and the incident angles of multiple light sources with respect to the light tracking panel.

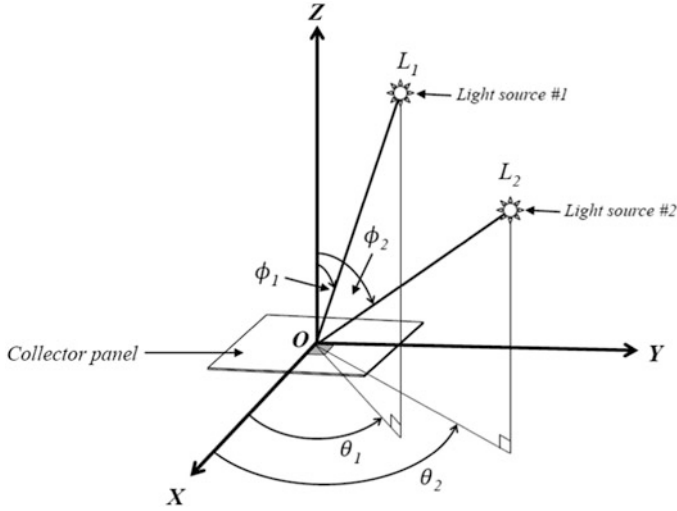


Fig. 2.6 Light vectors described in spherical coordinate system centered at the collector panel

2.4.2 Light Vectors in Spherical Coordinate System

Radiant energy from artificial lights such as fluorescent tubes can be similarly modeled as a point source or a line source. If the light emitter is modeled as a line source, the illuminance will vary with the reciprocal of the distance r for a bounded range $r_{i1} < r_i < r_{i2}$.

To express the analytical steps as a general rule, radiant energy from artificial source is modeled as a light ray coming from a point source.

Since the illuminance depends on the angle of incidence of the incoming light and the distance of the emitter from the receiver, it is more intuitive to model the artificial light ray vector using spherical coordinate system as shown in Fig. 2.6. In spherical coordinate system, a point is specified using the radial distance of that point from the origin, the polar angle ϕ measured from the zenith axis, and the azimuth angle θ which is orthogonal to the zenith axis.

2.5 Compound Homogeneous Transformation

In the derivation of tracking formula, it is important to describe the coordinate of the target (light sources) and the tracker. Both the target and the tracker can be static or moving. In the case of a Sun energy collector system, the target is moving while the tracker is usually fixed to the ground. In the case of an indoor robot feeding voltage or electric current from fluorescent lights, the targets are static while the tracker is moving. To describe the motion of both the target and the tracker, it is necessary to

define them in proper coordinate frames, the Earth-centered frame, the Earth-surface frame and the collector panel frame. The motion of the light ray that is described in one frame can be transformed to the collector panel frame for tracking purpose.

The previous Sun-tracking formulas [2, 3] are only applicable for a ground-fixed tracker tracing the Sunlight. The formulas only involve rotation transformation since there is no translating motion of the tracker itself.

This section is dedicated to the description of the technique used in coordinate transformation. The technique described here takes into account the offset position of the tracker from the reference point on the ground which requires a translational transformation in addition to rotational transformation. This is useful for the application of photovoltaic-powered rovers and robots.

For single-source tracking purpose, the coordinate transformation of a position vector \mathbf{r} between two frames, A and B , for a fixed tracker generally takes the form of:

$${}^A\mathbf{r} = {}^A R_B {}^B\mathbf{r} \quad (2.5)$$

where R is the rotation matrix that transforms the vector \mathbf{r} from B -frame to A -frame.

A tracking collector that is installed on a moving platform (e.g., rovers, robots), however, requires a coordinate transformation that involves translation of the platform as well. The coordinate transformation of a position vector \mathbf{r} between two frames, A and B , for a *mobile* tracker takes the general form of

$${}^A\mathbf{r} = {}^A R_B {}^B\mathbf{r} + {}^A\mathbf{d}_B \quad (2.6)$$

where ${}^A\mathbf{d}_B$ is the 3-by-1 Cartesian vector denoting the origin of frame B from the origin of frame A . It represents the distance of the tracker's center from a fixed reference point [5].

The rotation matrix and the translation vector in Eq. (2.6) can be combined into a single 4-by-4 matrix ${}^A T_B$ called the homogeneous transformation matrix:

$${}^A T_B = \begin{pmatrix} r_{11} & r_{12} & r_{13} & d_1 \\ r_{21} & r_{22} & r_{23} & d_2 \\ r_{31} & r_{32} & r_{33} & d_3 \\ 0 & 0 & 0 & 1 \end{pmatrix} = \begin{pmatrix} {}^A R_B & {}^A\mathbf{d}_B \\ \mathbf{0} & 1 \end{pmatrix} \quad (2.7)$$

The upper left 3-by-3 submatrix ${}^A R_B$ denotes the orientation of a frame B with respect to the frame A . The upper right 3-by-1 submatrix ${}^A\mathbf{d}_B$ denotes the position of the origin of frame B relative to frame A . The lower left 1-by-3 zero matrix denotes a perspective transformation, and the lower right element is a scaling factor which in this case is one (no scaling).

Since the homogeneous transformation matrix is a 4-by-4 matrix, a vector needs to be represented as a 4-by-1 vector for compatibility. The homogeneous coordinate expression for such vector can be represented by adding the scaling factor 1 as the

fourth element. Therefore, a vector $\mathbf{r} = (x \ y \ z)^T$ can equally be expressed as a homogeneous vector as follows

$$\mathbf{r}_{4 \times 1} = \begin{pmatrix} \mathbf{r}_{3 \times 1} \\ 1 \end{pmatrix} = \begin{pmatrix} x \\ y \\ z \\ 1 \end{pmatrix} \quad (2.8)$$

Using the homogeneous transformation matrix and the homogeneous representation of a vector, Eq. (2.6) can now be rewritten more concisely as

$$\begin{aligned} {}^A\mathbf{r} &= {}^A R_B {}^B\mathbf{r} + {}^A\mathbf{d}_B \\ &= \begin{pmatrix} {}^A R_B & {}^A\mathbf{d}_B \\ \mathbf{0} & 1 \end{pmatrix} (\mathbf{r}_{4 \times 1}) = \begin{pmatrix} r_{11} & r_{12} & r_{13} & d_1 \\ r_{21} & r_{22} & r_{23} & d_2 \\ r_{31} & r_{32} & r_{33} & d_3 \\ 0 & 0 & 0 & 1 \end{pmatrix} \begin{pmatrix} x \\ y \\ z \\ 1 \end{pmatrix} \\ &= {}^A T_B {}^B\mathbf{r} \end{aligned} \quad (2.9)$$

More complete references on the properties of homogeneous transformation matrix can be found in Jazar [6] and Legnani [7]. Three of the important properties pertaining to the application in this work are reviewed here.

1. Decomposition of Homogeneous Transformation Matrix

The homogeneous transformation matrix ${}^A T_B$ can be decomposed to matrix product of a translation matrix ${}^A D_B$ and a rotation matrix ${}^A R_B$:

$$\begin{aligned} {}^A T_B &= {}^A D_B {}^A R_B \\ &= \begin{pmatrix} 1 & 0 & 0 & d_x \\ 0 & 1 & 0 & d_y \\ 0 & 0 & 1 & d_z \\ 0 & 0 & 0 & 1 \end{pmatrix} \begin{pmatrix} r_{11} & r_{12} & r_{13} & 0 \\ r_{21} & r_{22} & r_{23} & 0 \\ r_{31} & r_{32} & r_{33} & 0 \\ 0 & 0 & 0 & 1 \end{pmatrix} \end{aligned} \quad (2.10)$$

As Eq. (2.10) shows that the order of transformation is done by performing a pure rotation followed by a pure translation. The product of the matrices is not interchangeable

$${}^A T_B = {}^A D_B {}^A R_B \neq {}^A R_B {}^A D_B. \quad (2.11)$$

Corollary of the decomposition rule, the homogeneous transformation matrix can be modified to function as a pure translation matrix

$${}^A T_B = {}^A D_B = \begin{pmatrix} 1 & 0 & 0 & d_x \\ 0 & 1 & 0 & d_y \\ 0 & 0 & 1 & d_z \\ 0 & 0 & 0 & 1 \end{pmatrix} \quad (2.12)$$

or a pure rotation matrix

$${}^A T_B = {}^A R_B = \begin{pmatrix} r_{11} & r_{12} & r_{13} & 0 \\ r_{21} & r_{22} & r_{23} & 0 \\ r_{31} & r_{32} & r_{33} & 0 \\ 0 & 0 & 0 & 1 \end{pmatrix} \quad (2.13)$$

2. Inverse Homogeneous Transformation Matrix

Given the homogeneous transformation matrix from a frame B to a frame A

$${}^A T_B = \begin{pmatrix} {}^A R_B & {}^A \mathbf{d}_B \\ \mathbf{0} & 1 \end{pmatrix} \quad (2.14)$$

the homogeneous transformation matrix from the frame A to the frame B can be obtained by inverting the matrix ${}^A T_B$

$${}^B T_A = {}^A T_B^{-1} = \begin{pmatrix} {}^A R_B & {}^A \mathbf{d}_B \\ \mathbf{0} & 1 \end{pmatrix}^{-1} = \begin{pmatrix} {}^A R_B^T & -{}^A R_B^T {}^A \mathbf{d}_B \\ \mathbf{0} & 1 \end{pmatrix} \quad (2.15)$$

Unlike rotation matrix in orthogonal frames, the homogeneous transformation matrix is not orthogonal; hence, its inverse is not equal to its transpose

$${}^A T_B^{-1} \neq {}^A T_B^T. \quad (2.16)$$

3. Compound Homogeneous Transformation Matrix

Transforming body coordinates between more than two frames can be done with successive homogeneous transformation matrices. For example, if the homogeneous transformation matrix from frame A to frame B , and another transformation matrix to from frame B to frame C are

$${}^B T_A = \begin{pmatrix} {}^B R_A & {}^B \mathbf{d}_A \\ \mathbf{0} & 1 \end{pmatrix} \quad {}^C T_B = \begin{pmatrix} {}^C R_B & {}^C \mathbf{d}_B \\ \mathbf{0} & 1 \end{pmatrix} \quad (2.17)$$

then transformation of body coordinates from frame A to frame C can be completed with a single homogeneous transformation matrix by multiplying ${}^B T_A$ and ${}^C T_B$ in order

$${}^C T_A = {}^C T_B {}^B T_A \quad (2.18)$$

2.6 Coordinate Frames and Transformation

The primary objective of tracking is to rotate the collector panel such that its normal vector $\hat{\mathbf{n}}$ is along the resultant light vector. The three main components in our tracking system—the light source(s), the tracking collector panel, and the body that is carrying the tracker—are more conveniently defined with each respective reference frame. For example, the Sun movement can be modeled in an Earth-centered frame, while the orientation of the collector panel is more appropriately defined with a reference frame that is centered on its rotation axes. The coordinate frames pertaining to these components need to be defined and transformation matrix is required to transfer geometrical and kinematical information between the frames.

2.6.1 Earth-Centered Frame E

The Sun vector for solar tracking purposes is most conveniently defined in the Earth-centered frame. Its position vector can be defined in the Earth-centered frame E as a 3-by-1 vector as

$${}^E\mathbf{S} = \begin{pmatrix} \cos \delta \cos \omega \\ -\cos \delta \sin \omega \\ \sin \delta \end{pmatrix} \quad (2.19)$$

where δ is the declination angle and ω is the hour angle in the Earth-centered coordinate frame.

2.6.2 Earth-Surface Frame S

To make the \mathbf{S} -vector useful, a transformation from the Earth-centered frame E to the Earth-surface is required. To do this, a frame S is attached at a point O_S on the Earth surface with a distance R_0 from the center of the Earth. The x_S -axis is always oriented towards North, the y_S -axis points West, and the z_S is defined as the zenith axis. The origin of the frame O_S is located at a longitude ϕ and latitude λ . The distance vector ${}^S\mathbf{d}$ is then expressed as

$${}^S\mathbf{d} = \begin{pmatrix} 0 \\ 0 \\ R_0 \end{pmatrix} \quad (2.20)$$

and the rotation matrix from the E -frame to the S -frame is

$${}^S R_E = R_{z,\pi} R_{y,\pi/2-\lambda} R_{z,\phi} = \begin{pmatrix} -\cos \phi \sin \lambda & -\sin \phi \sin \lambda \cos \lambda \\ \sin \phi & -\cos \phi & 0 \\ \cos \phi \cos \lambda & \sin \phi \cos \lambda & \sin \lambda \end{pmatrix} \quad (2.21)$$

Therefore, the transformation matrix from the Earth-centered E -frame and to the Earth-surface S -frame, therefore, is expressed as

$${}^S T_E = \begin{pmatrix} {}^S R_E & {}^S \mathbf{d} \\ 0 & 1 \end{pmatrix} = \begin{pmatrix} -\cos \phi \sin \lambda & -\sin \phi \sin \lambda \cos \lambda & 0 \\ \sin \phi & -\cos \phi & 0 & 0 \\ \cos \phi \cos \lambda & \sin \phi \cos \lambda & \sin \lambda & R_0 \\ 0 & 0 & 0 & 1 \end{pmatrix} \quad (2.22)$$

Now, the 4-by-1 Sun vector can be expressed in the Earth-surface frame S as

$${}^S \mathbf{S} = {}^S T_E {}^E \mathbf{S} \quad (2.23)$$

The distance ${}^S \mathbf{d}$ can be assumed to be zero for Sun-tracking purpose. However, the formula here is treated generally to include satellite tracking where the relative distance of the satellite with the center of the Earth and the tracker's position are important. For solar tracking purpose, R_0 can be considered as zero.

2.6.3 Collector-Centered Frame C

The coordinate frame for the collector panel is shown in Fig. 2.7. The collector is assumed to have an arbitrary orientation with respect to the surface of the Earth. It is assumed also that the distance between the origin of the collector-centered C -frame O_C and the origin of the Earth-surface S -frame O_S is negligible; hence, their origins are coincident. The z_C -axis is defined along the direction of the normal of the collector plane, and the x_C - y_C plane is defined as the panel's surface plane. Initially, it is assumed that the orientation of the C -frame is parallel to the Earth-surface S -frame.

1. Tip-Roll Dual Axis Tracker

To point the normal of the collector panel to the light vector, the C -frame is turned from a coincident orientation with the S -frame about the y_C -axis (primary axis for the tip-tilt configuration) by $-\alpha$ degrees and then it is turned about the x_C -axis (secondary axis for the tip-roll configuration) by $-\beta$ degrees. Since both

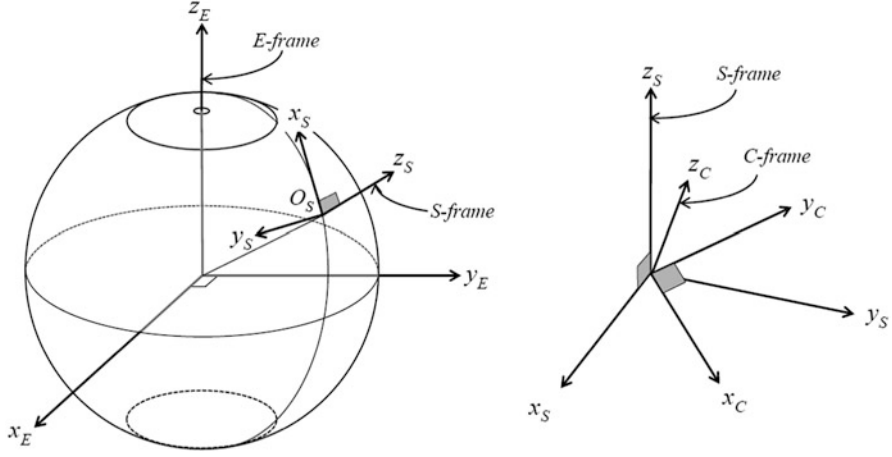


Fig. 2.7 Orientation of the panel-fixed C -frame with respect to the Earth-surface S -frame and the Earth-centered E -frame for a ground-fixed tracker

frames share the same origin, only rotation matrix is required to transform from the S -frame to the C -frame:

$$\begin{aligned}
 {}^C R_S &= R_{x, -\beta} R_{y, -\alpha} = \begin{pmatrix} 1 & 0 & 0 \\ 0 & \cos \beta & -\sin \beta \\ 0 & \sin \beta & \cos \beta \end{pmatrix} \begin{pmatrix} \cos \alpha & 0 & \sin \alpha \\ 0 & 1 & 0 \\ -\sin \alpha & 0 & \cos \alpha \end{pmatrix} \\
 &= \begin{pmatrix} \cos \alpha & 0 & \sin \alpha \\ \sin \beta \sin \alpha & \cos \beta & -\sin \beta \cos \alpha \\ -\cos \beta \sin \alpha & \sin \beta & \cos \beta \cos \alpha \end{pmatrix} \quad (2.24)
 \end{aligned}$$

Therefore the transformation matrix for a ground-fixed, tip-roll dual axis tracker becomes

$${}^C T_S = \begin{pmatrix} \cos \alpha & 0 & \sin \alpha & 0 \\ \sin \beta \sin \alpha & \cos \beta & -\sin \beta \cos \alpha & 0 \\ -\cos \beta \sin \alpha & \sin \beta & \cos \beta \cos \alpha & 0 \\ 0 & 0 & 0 & 1 \end{pmatrix} \quad (2.25)$$

2. Azimuth-Elevation Dual Axis Tracker

For azimuth-elevation configuration, the C -frame is turned from a coincident orientation with the S -frame about its primary z_C -axis by $-\alpha$ degrees, and then about its secondary x_C -axis by $-\beta$ degrees. The rotation matrix is required to transform from the S -frame to the C -frame in the azimuth-elevation configuration

$$\begin{aligned}
{}^C R_S &= R_{x,-\beta} R_{z,-\alpha} = \begin{pmatrix} 1 & 0 & 0 \\ 0 & \cos \beta & -\sin \beta \\ 0 & \sin \beta & \cos \beta \end{pmatrix} \begin{pmatrix} \cos \alpha & -\sin \alpha & 0 \\ \sin \alpha & \cos \alpha & 0 \\ 0 & 0 & 1 \end{pmatrix} \\
&= \begin{pmatrix} \cos \alpha & -\sin \alpha & 0 \\ \cos \beta \sin \alpha & \cos \beta \cos \alpha & -\sin \beta \\ \sin \beta \sin \alpha & \sin \beta \cos \alpha & \cos \beta \end{pmatrix} \quad (2.26)
\end{aligned}$$

Therefore the transformation matrix for a ground-fixed, azimuth-elevation dual axis tracker becomes

$${}^C T_S = \begin{pmatrix} \cos \alpha & -\sin \alpha & 0 & 0 \\ \cos \beta \sin \alpha & \cos \beta \cos \alpha & -\sin \beta & 0 \\ \sin \beta \sin \alpha & \sin \beta \cos \alpha & \cos \beta & 0 \\ 0 & 0 & 0 & 1 \end{pmatrix} \quad (2.27)$$

The rotation matrices for a tilt-roll and an azimuth-elevation configurations are presented here. For any other dual axis tracker configuration, Appendix provides the list of local frame rotation matrices to transform the coordinates from the Earth-surface frame S to the collector panel frame C .

2.6.4 Moving Platform Body Frame B

In case of mobile trackers where the tracker is installed on a moving platform such as a vehicle, or a robot, another body-fixed frame needs to be defined to take into account the translational and rotational motions of the platform. Its origin O_B is assumed to coincide with the origin of the collector-centered C -frame. The distance of the shared origin from the Earth-surface fixed reference point O_S is described by a vector ${}^B \mathbf{d}$

$${}^S \mathbf{d} = \begin{pmatrix} d_x \\ d_y \\ 0 \\ 1 \end{pmatrix} \quad (2.28)$$

as it is moving on the x - y plane only. Figure 2.8 illustrates the coordinate frames. Assuming the movement of the platform is much less than the radius of the Earth, the platform can be considered as translationally static while tracking the Sun. For the case of artificial light tracking, the distance of the collector to the sources of light is important. For Sun-tracking purpose, the distance vector ${}^B \mathbf{d}$ can practically be considered zero.

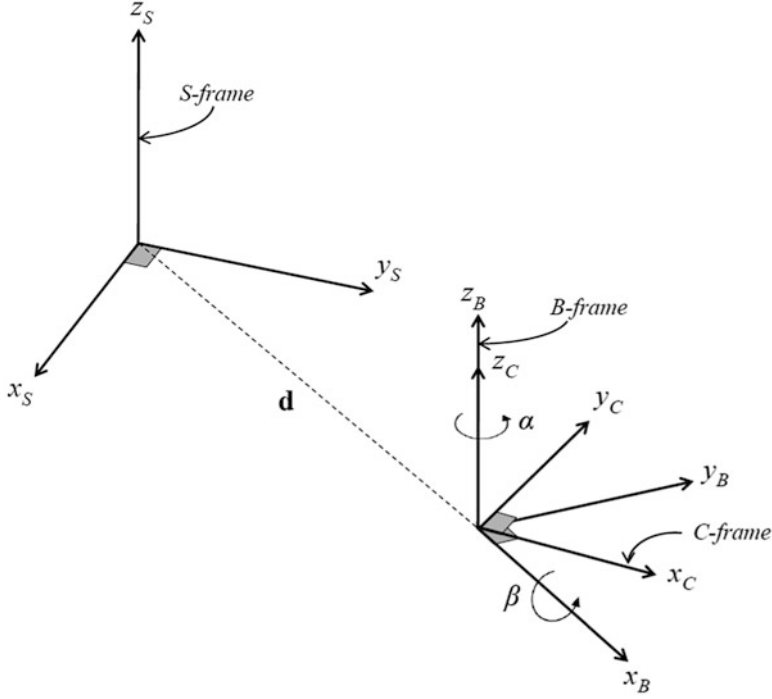


Fig. 2.8 Orientation of the platform-fixed B -frame and the panel-fixed C -frame with respect to the Earth-surface S -frame for a mobile tracker

The B -frame's orientation is assumed to be parallel to the orientation of the Earth-surface S -frame initially with its x_B -axis pointing North, the y_B -axis pointing West, and the z_B -axis in the zenith direction. The platform body frame B rotates about its z_B -axis by γ degrees. Thus, its transformation matrix is expressed as

$${}^B T_S = \begin{pmatrix} {}^B R_S & {}^B \mathbf{d} \\ 0 & 1 \end{pmatrix} = \begin{pmatrix} \cos \gamma & \sin \gamma & 0 & d_x \\ -\sin \gamma & \cos \gamma & 0 & d_y \\ 0 & 0 & 1 & 0 \\ 0 & 0 & 0 & 1 \end{pmatrix} \quad (2.29)$$

Therefore, for a collector-frame C in B in tip-roll configuration, the transformation matrix from S -frame to C -frame becomes

$$\begin{aligned} {}^C T_S &= {}^C T_B {}^B T_S \\ &= \begin{pmatrix} c\alpha c\gamma & c\alpha s\gamma & s\alpha & d_x \\ s\beta s\alpha c\gamma - c\beta s\gamma & s\beta s\alpha s\gamma + c\beta c\gamma & -s\beta c\alpha & d_y \\ -s\alpha c\beta c\gamma - s\beta s\gamma & -s\alpha c\beta s\alpha + s\beta c\gamma & c\beta c\alpha & 0 \\ 0 & 0 & 0 & 1 \end{pmatrix} \end{aligned} \quad (2.30)$$

For azimuth-elevation configuration, the transformation matrix from S -frame to C -frame is

$${}^C T_S = {}^C T_B {}^B T_S$$

$$= \begin{pmatrix} \cos \alpha + \gamma & -\sin \alpha + \gamma & 0 & d_x \\ \cos \beta \sin \alpha + \gamma & \cos \beta \cos \alpha + \gamma & -\sin \beta & d_y \\ \sin \beta \sin \alpha + \gamma & \sin \beta \cos \alpha + \gamma & \cos \beta & 0 \\ 0 & 0 & 0 & 1 \end{pmatrix} \quad (2.31)$$

2.7 Example

A mobile robot carrying photovoltaic panels is moving across the floor of an indoor environment which is lit by several artificial lights attached on the ceiling. The panels orientation is controlled by a light-tracking that points the direction of the brightest illuminance. As the photovoltaic panel is translating across the room, the tracker has to actively find the brightest illuminance based on its relative position with respect to the light sources.

2.7.1 Trajectory Constraint

The indoor environment is assumed to be a room of 20m in length and 10m in width, with the height of a standard office room's ceiling which is approximately 2.5m. Six light emitters modelled as point sources are positioned uniformly as shown in Fig. 2.9.

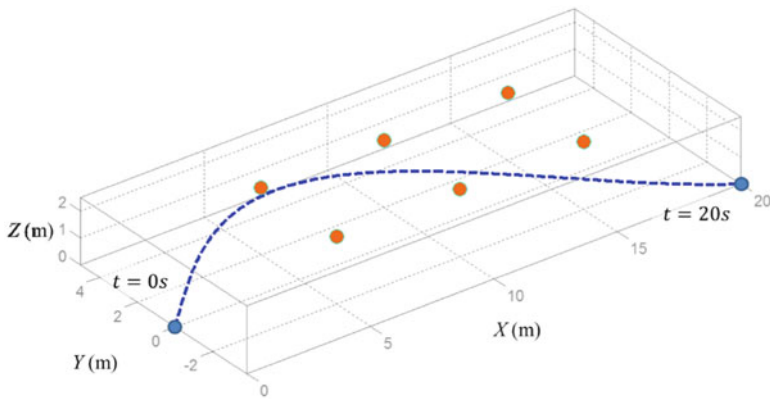
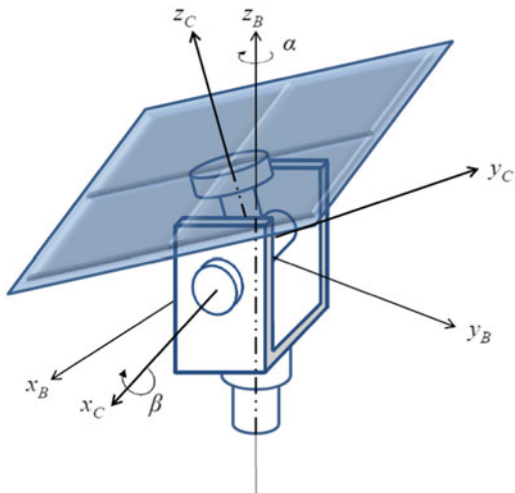


Fig. 2.9 An indoor environment with six ceiling-fixed light emitters and the path for the mobile tracker. The duration from the starting to the end point is 20 s

Fig. 2.10 Dual-axis light tracker configuration used in this example



To illustrate the light-tracking motion and the requirement for the directional control system, a path for the vehicle is defined a priori. The vehicle is to follow the path at a constant speed while maintaining its direction parallel to the tangent of the path line.

2.7.2 Dual-Axis Tracker

A conceptual illustration of the dual-axis tracking system is shown in Fig. 2.10. The mechanism is similar to an azimuth-altitude solar tracker which has its primary axis vertical to the local, body-frame of the vehicle which is called the azimuth or the yaw axis, and a secondary axis normal to the primary axis which is referred to as the elevation or the pitch axis. These two axes intersect at the wrist point. The orientation of the face of the panel is directed by two independent rotary actuators which control the yaw angle α and the pitch angle β . The amount of angular displacements and velocities depends on the panel's relative position with respect to the light emitters and the speed of the vehicle.

2.7.3 Reference Frames

We define a global reference frame G that is attached at a fixed reference point in the room with its X - Y plane describing the floor and the Z -axis pointing towards the ceiling. The positions of the light emitters and the mobile robot will be referred to this reference frame. A body-fixed frame, B , is attached to the vehicle which is moving in the G -frame. The light vectors are calculated in the B -frame in terms of

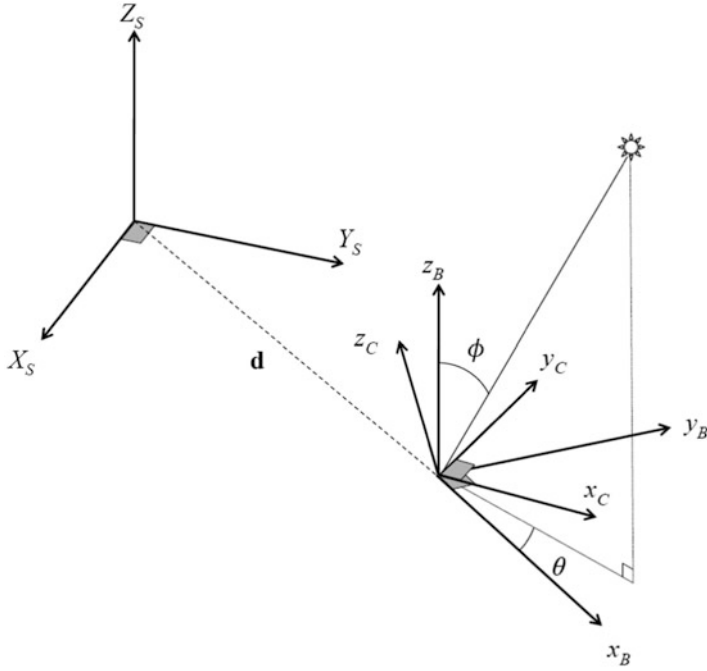


Fig. 2.11 Reference frames association for a mobile light-tracker. The vehicle body-fixed B -frame has a translation distance of d and a rotation angle of γ about the global Z -axis. The collector panel-fixed C -frame shares the same origin as the B -frame

azimuth angle θ and elevation angle ϕ , which would define their angles of incidence on the vehicle. Another body-frame C is attached to the mobile robot, sharing the same origin with B and follows the orientation of the vehicle, which is denoted by the angle γ about the z_B -axis. The input angles for both axes of the tracker are defined in this reference frame based on the azimuth and elevation angles expressed in B . These reference frames are depicted in Fig. 2.11.

The problem can be stated as the following: given the vehicle's position and its orientation with respect to a fixed, global reference frame, what are the angular displacements needed by the rotary actuators of the tracker to orient the photovoltaic panel to the direction of the brightest illuminance from an arbitrary panel orientation?

2.7.4 Computing the Illuminance Received by Collector Panel

Equation (2.4) is used as the basis in computing the illuminance received by the collector panel on the moving robot. The light intensity I_i of each source is assumed to be of a unit magnitude. Since the collector panel is moving, the illuminance received E is dependent on the position (distance) and the angle of incident of the

light sources with respect to the collector panel orientation. The position of the i th source at time t is recorded as $\mathbf{r}_i(t)$ and the pointing direction of the panel is recorded as $\mathbf{n}(t)$.

A step-by-step procedure for the algorithm is detailed as below:

1. Define the position vector of the light source in its natural frame (Earth-centered frame E for Sun tracking and the Earth-surface frame S for ground-fixed artificial light sources). For example, the position of an artificial light in an indoor environment is defined as a vector \mathbf{r} in $G(^G\mathbf{r})$

$$^G\mathbf{r} = \text{position vector of light source as seen in } G \quad (2.32)$$

2. The body carrying the collector panel is assumed to be translating across the room on a prescribed path. To find the light position with respect to the body at a particular position in the G -frame, transform the vector \mathbf{r} in the body-fixed frame B using the homogeneous transformation matrix $^B T_G$

$$^B\mathbf{r} = ^B T_G ^G\mathbf{r} \quad (2.33)$$

3. Assuming the collector-centered frame C is different from the B -frame, another transformation is done to express the vector \mathbf{r} in the C -frame

$$^C\mathbf{r} = ^C T_B ^B\mathbf{r} = ^C T_B ^B T_G ^G\mathbf{r} \quad (2.34)$$

4. The vector $^C\mathbf{r}$ is expressed in the Cartesian coordinates (x, y, z) . The vector is transformed into spherical coordinates (r, θ, ϕ)

$$^C\mathbf{r} = \begin{pmatrix} x \\ y \\ z \end{pmatrix} \rightarrow \begin{pmatrix} r \\ \theta \\ \phi \end{pmatrix} \quad (2.35)$$

5. Define the pointing direction of the collector panel n in terms of a unit vector in spherical coordinates to reduce the variables from the Cartesian coordinates x , y , and z to two angle variables as only the direction of the panel is concerned. As the distance is not of importance, the radial distance can be defined as 1

$$\hat{\mathbf{n}} = \begin{pmatrix} 1 \\ \alpha \\ \beta \end{pmatrix} \quad (2.36)$$

6. To find the optimum orientation n that would receive the most illumination from the light source, Eq. (2.4) is used. Since the variables in this equation are α (yaw angle) and β (pitch angle) only, a 3D plot of illuminance E vs. α vs. β can be used to find the best $[\alpha^* \beta^*]$ pair that gives the largest E value:

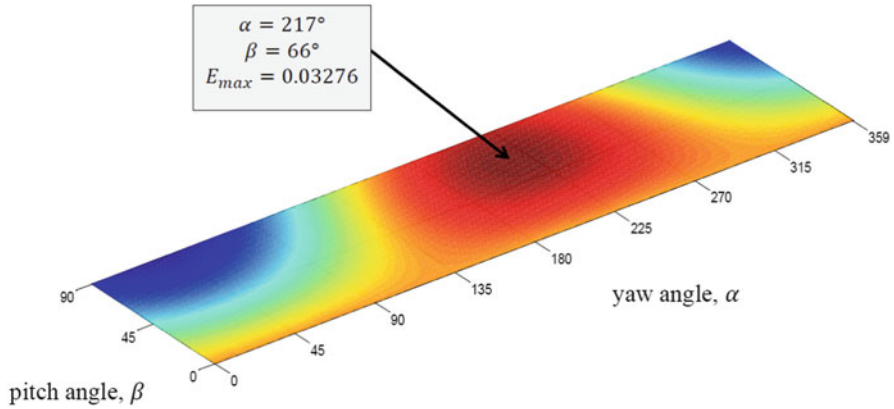


Fig. 2.12 A three-dimensional plot of illuminance, E vs. azimuth angle, α vs. pitch angle, β . For Example 1, the collector panel receives the brightest illuminance at the instance $t = 9$ s when its azimuth angle is 277° and its pitch angle is 66°

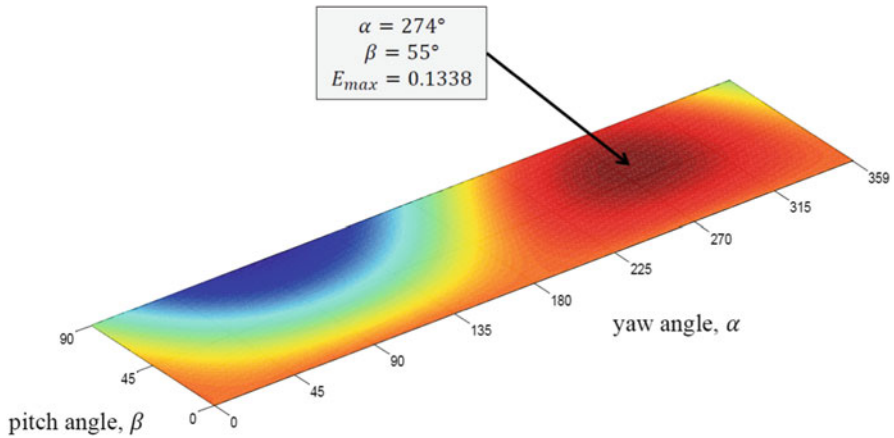


Fig. 2.13 A three-dimensional plot of illuminance, E vs. azimuth angle, α vs. pitch angle, β . For Example 2, the collector panel receives the brightest illuminance at the instance $t = 9$ s when its azimuth angle is 274° and its pitch angle is 55°

$$E = \sum_i^n \frac{1}{r_i^2} c \hat{\mathbf{n}} \cdot c \hat{\mathbf{r}}_i$$

Note that E is just a quantification of the intensity of the light received, not illumination in photometric. Examples of the 3D plot are shown in Figs. 2.12 and 2.13.

7. These steps are repeated for each new point in the prescribed path and the history of $[\alpha^* \beta^*]$ is recorded for every point.

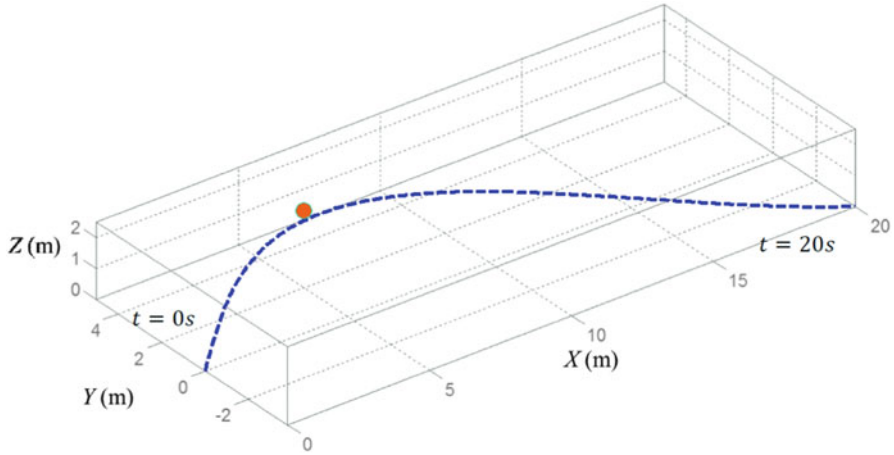


Fig. 2.14 An indoor environment with a ceiling-fixed light emitter and the path for the mobile tracker. The duration from the starting to the end point is 20 s

2.7.5 Example 1

Let us consider a simple problem where the room is lit by one artificial light at point ${}^G L = [5.0 \ 2.0 \ 2.5]^T$ as shown in Fig. 2.14. To use this information and to transform the light vector ${}^G L$ to the collector panel frame, we need to perform three coordinate transformations: from the G -frame (${}^G L$) to the vehicle's B -frame (${}^B L$) to the collector panel's C -frame (${}^C L$). Following Eq. (2.31), the homogeneous transformation matrix can be expressed as

$$\begin{aligned}
 {}^C L &= {}^C T_B {}^B T_G {}^G T^G L \\
 &= \begin{pmatrix} \cos \alpha + \gamma & -\sin \alpha + \gamma & 0 & X \\ \cos \beta \sin \alpha + \gamma & \cos \beta \cos \alpha + \gamma & -\sin \beta & Y \\ \sin \beta \sin \alpha + \gamma & \sin \beta \cos \alpha + \gamma & \cos \beta & 0 \\ 0 & 0 & 0 & 1 \end{pmatrix} \begin{pmatrix} 5.0 \\ 2.0 \\ 2.5 \\ 1 \end{pmatrix} \quad (2.37)
 \end{aligned}$$

where $d_x(t)$ and $d_y(t)$ are the positions of the vehicle in the G -frame, as shown in Fig. 2.15, and $\gamma(t)$ is the vehicle's orientation with respect to the G -frame, as shown in Fig. 2.16. These quantities are known as the vehicle's path is prescribed.

The time histories of the yaw angle $\alpha(t)$ and the pitch angle $\beta(t)$ for the tracker under a single artificial light are shown in Figs. 2.17 and 2.18. Figure 2.12 shows an example of illuminance received by the collector panel as a function of yaw angle and pitch angle at time $t = 9$ s. As shown in Fig. 2.19, the illuminance received by a dual-axis tracker is significantly higher compared to a non-tracking, zenith-fixed collector panel.

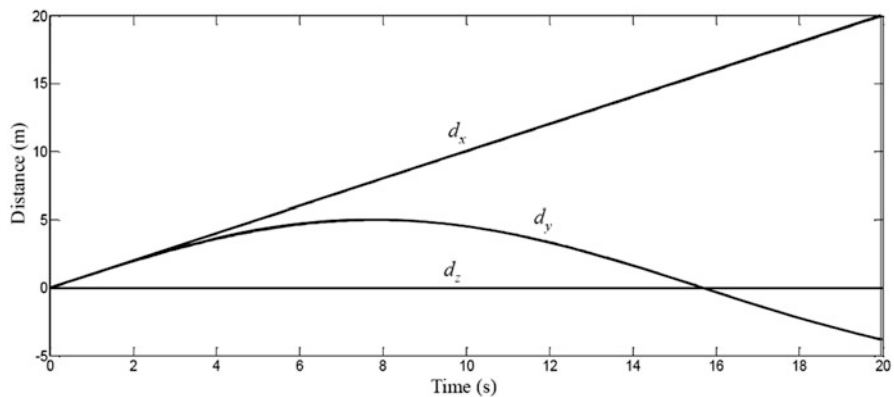


Fig. 2.15 Position of the mobile tracker with respect to the global frame in x , y , and z -direction over time

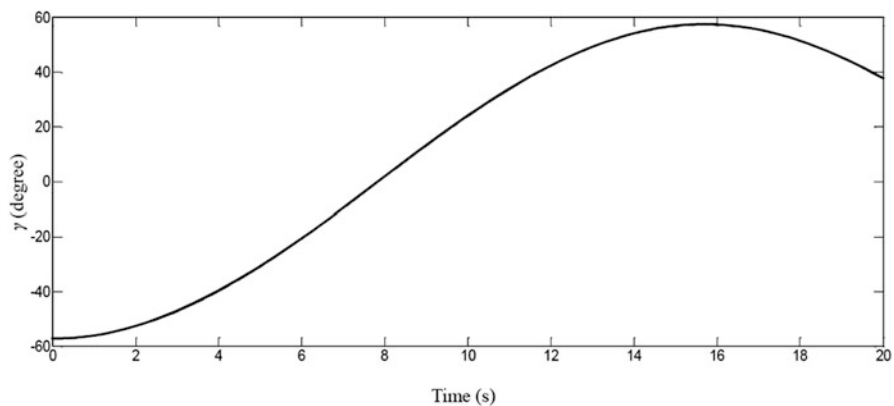


Fig. 2.16 Orientation of the mobile tracker with respect to the global frame γ (degree) vs. time (second)

2.7.6 Example 2

We assume the tracker is equipped on a moving vehicle under multiple lighting as shown in Fig. 2.9. The positions of the six lights are:

$${}^G L_1 = [5.0 \ 2.0 \ 2.5]^T$$

$${}^G L_2 = [5.0 \ 2.0 \ 2.5]^T$$

$${}^G L_3 = [10 \ 2.0 \ 2.5]^T$$

$${}^G L_4 = [10 \ -2 \ 2.5]^T$$

Fig. 2.17 Yaw angle α (degree) vs. time (second) for the single light emitter case

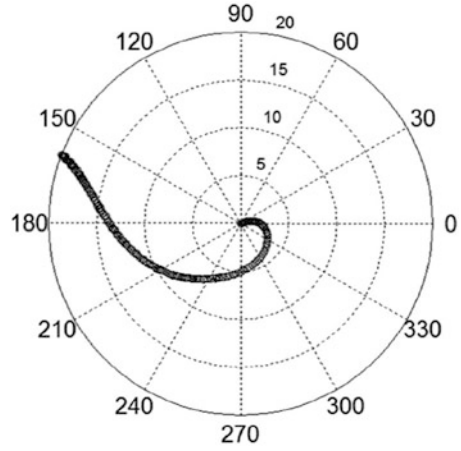
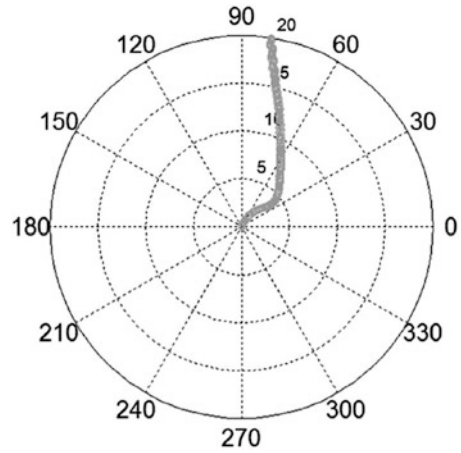


Fig. 2.18 Pitch angle β (degree) vs. time (second) for the single light emitter case



$${}^G L_5 = [10 \ 2 \ 2.5]^T$$

$${}^G L_6 = [15 \ -2 \ 2.5]^T$$

As the vehicle is moving across the room, the light intensity received by the collector panel is varying; therefore, the panel's orientation cannot be a function of the fixed positions of the lights. At each discrete point of the vehicle's path, \mathbf{d} , each light position is calculated and the direction of the brightest illumination is denoted by $\hat{\mathbf{n}}(t)$ which maximizes Eq. (2.4)

$$\max E_r(t) = \sum_i^n \frac{1}{r_i^2(t)} \hat{\mathbf{n}}(t) \cdot \hat{\mathbf{r}}_i(t) \quad (2.38)$$

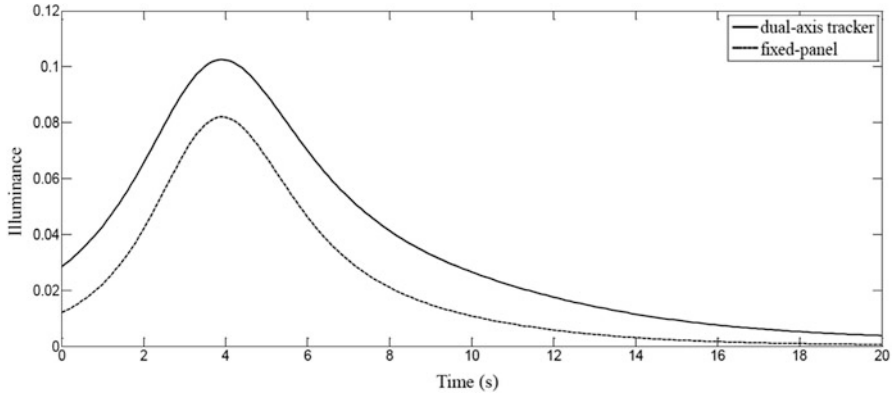
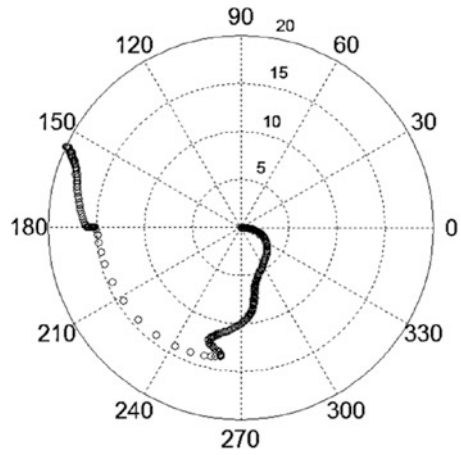


Fig. 2.19 Comparison of the brightness (illumination) received for a fixed panel and a tracking panel for the single light emitter case

Fig. 2.20 Yaw angle α (degree) vs. time (second) for the multiple light emitters case



Prior to finding the vector $\hat{\mathbf{n}}(t)$ (Step 5), each light vector ${}^G\mathbf{r}_i$ needs to be rotated to the collector panel's frame C

$$\begin{aligned}
 {}^C\mathbf{r}_i &= {}^C T_B {}^B T_G {}^G T^G \mathbf{r}_i \\
 &= \begin{pmatrix} \cos \alpha + \gamma & -\sin \alpha + \gamma & 0 & 0 \\ \cos \beta \sin \alpha + \gamma & \cos \beta \cos \alpha + \gamma & -\sin \beta & 0 \\ \sin \beta \sin \alpha + \gamma & \sin \beta \cos \alpha + \gamma & \cos \beta & 0 \\ 0 & 0 & 0 & 1 \end{pmatrix} {}^G\mathbf{r}_i \quad (2.39)
 \end{aligned}$$

where $d_x(t)$ and $d_y(t)$ are the known positions of the vehicle in the G -frame (Fig. 2.15), and $\gamma(t)$ is the vehicle's orientation with respect to the G -frame (Fig. 2.16).

Fig. 2.21 Pitch angle β (degree) vs. time (second) for the multiple light emitters case

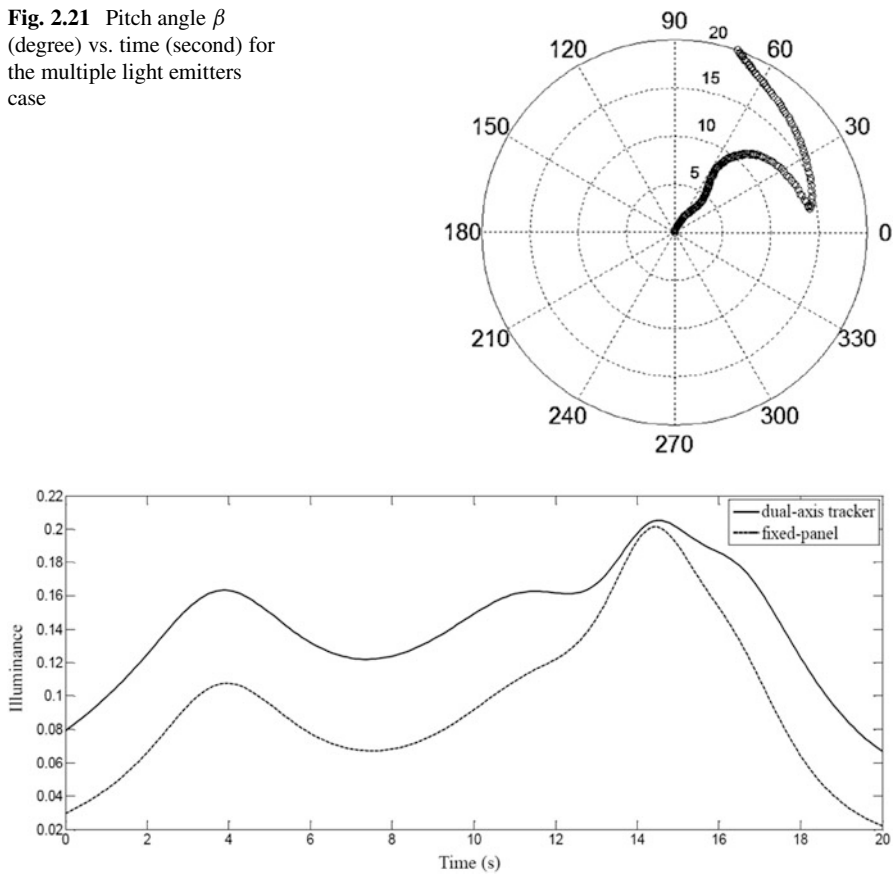


Fig. 2.22 Comparison of the brightness (illumination) received for a fixed panel and a tracking panel for the multiple light emitters case

The time histories of the yaw angle α and the pitch angle β for the tracker under multiple lights condition are shown in Figs. 2.20 and 2.21. Figure 2.13 shows an example of illuminance received by the collector panel as a function of yaw angle and pitch angle at time $t = 9$ s. Figure 2.22 shows that the dual-axis tracker collects significantly more illuminance in the multi-light environment compared to a fixed-panel.

2.8 Conclusions

The general light-tracking formula for generating power from radiation has been derived using compound homogeneous transformation method. The newly derived formula is more general mathematical solution for any dual-axis light tracker

as it can be applied to trackers on mobile platforms such as rovers and robots. The formula can also be employed on any conventional Sun-trackers and for indoor environment implementing orientatable photovoltaic modules. The formula, however, is limited for platforms moving on a smooth, two-dimensional plane.

The following suggestions may be included in the future studies of tracking system:

1. A three-dimensional translation motion for the mobile platform for the application of rovers in an uneven terrain. The derivation of the formula must take into account the pitching and rolling motion of the vehicle itself to orient its photovoltaic panels towards the radiance source.
2. Calculation of the light vector from extraterrestrial objects, such as Mars or Jupiter, for the application of a lunar rovers.
3. Sun-tracking formula as a function of Earth orbit elements for spacecraft application.

Appendix: Local Frame Double Rotation

The collector panel frame rotation matrices about local axes is presented in this appendix. The rotation matrix can be used for any six combination of primary and secondary axes to transform coordinates from the Earth-surface frame (global frame) to the collector panel frame (local frame). The angle about the primary axis is denoted by α and the angle about the secondary axis is denoted by β .

1. Primary: x -axis Secondary: y -axis

$$R_{y,-\beta} R_{x,-\alpha} = \begin{pmatrix} \cos \beta & \sin \alpha \sin \beta & \cos \alpha \sin \beta \\ 0 & \cos \alpha & -\sin \alpha \\ -\sin \beta & \cos \beta \sin \alpha & \cos \alpha \cos \beta \end{pmatrix} \quad (2.40)$$

2. Primary: x -axis Secondary: z -axis

$$R_{z,-\beta} R_{x,-\alpha} = \begin{pmatrix} \cos \beta - \cos \alpha \sin \beta & \sin \alpha \sin \beta \\ \sin \beta & \cos \alpha \cos \beta & -\cos \beta \sin \alpha \\ 0 & \sin \alpha & \cos \alpha \end{pmatrix} \quad (2.41)$$

3. Primary: y -axis Secondary: x -axis (tip-tilt configuration)

$$R_{x,-\beta} R_{y,-\alpha} = \begin{pmatrix} \cos \alpha & 0 & \sin \alpha \\ \sin \alpha \sin \beta & \cos \beta & -\cos \alpha \sin \beta \\ -\cos \beta \sin \alpha & \sin \beta & \cos \alpha \cos \beta \end{pmatrix} \quad (2.42)$$

4. Primary: y -axis Secondary: z -axis

$$R_{z,-\beta} R_{y,-\alpha} = \begin{pmatrix} \cos \alpha \cos \beta - \sin \beta \sin \alpha \cos \beta & & \\ \cos \alpha \sin \beta & \cos \beta & \sin \alpha \sin \beta \\ -\sin \alpha & 0 & \cos \alpha \end{pmatrix} \quad (2.43)$$

5. Primary: z -axis Secondary: x -axis (azimuth-elevation configuration)

$$R_{x,-\beta} R_{z,-\alpha} = \begin{pmatrix} \cos \alpha & -\sin \alpha & 0 \\ \cos \beta \sin \alpha & \cos \alpha \cos \beta - \sin \beta & \\ \sin \alpha \sin \beta & \cos \alpha \sin \beta & \cos \beta \end{pmatrix} \quad (2.44)$$

6. Primary: z -axis Secondary: y -axis

$$R_{y,-\beta} R_{z,-\alpha} = \begin{pmatrix} \cos \alpha \cos \beta & -\cos \beta \sin \alpha & \sin \beta \\ \sin \alpha & \cos \alpha & 0 \\ -\cos \alpha \sin \beta & \sin \alpha \sin \beta & \cos \beta \end{pmatrix} \quad (2.45)$$

Key Symbols

d	Translation scalar
\mathbf{d}	Translation vector
d_i	Element i of \mathbf{d}
D	Homogeneous translation matrix
${}^A D_B$	Homogeneous translation matrix from B -frame to A -frame
E	Total illumination
E_r	Distance-dependant illuminance
E_φ	Incident angle-dependant illuminance
I, I_i	Light intensity
$\hat{\mathbf{n}}$	Normal unit vector to the collector
O	Origin point of a coordinate frame
r	Distance between target and source of light, position scalar
\mathbf{r}	Position vector
r_i	Element i of \mathbf{r}
r_{ij}	Element of row i and column j of matrix R
${}^A \mathbf{r}$	Vector \mathbf{r} expressed in A -frame
$\hat{\mathbf{r}}$	Direction of light ray with respect to the collector
r, θ, ϕ	Local spherical coordinates
R	Rotation transformation matrix

${}^A R_B$	Rotation transformation matrix from B -frame to A -frame
$R_{x,\alpha}$	Rotation transformation about x -axis with α angle
S	Sun vector
T	Homogeneous transformation matrix
${}^A T_B$	Homogeneous transformation matrix from B -frame to A -frame
x, y, z	Local coordinate axes
X, Y, Z	Global coordinate axes
α	Yaw angle
β	Pitch angle
γ	Orientation of the vehicle body-frame with respect to the global frame
θ	Azimuth angle
ϕ	Elevation angle
φ	Angle of incidence

References

1. Bretagnon P, Francou G (1988) Planetary theories in rectangular and spherical variables—vsop87 solutions. *Astron Astrophys* 202(1–2):309–315
2. Chen Y, Chong K, Bligh T, Chen L, Yunus J, Kannan K, Lim B, Lim C, Alias M, Bidin N, Aliman O, Salehan S, Shk. Abd. Rezan SAH, Tam C, Tan K (2001) Non-imaging, focusing heliostat. *Sol Energy* 71(3):155–164
3. Chen Y, Lim B, Lim C (2006) General sun tracking formula for heliostats with arbitrarily oriented axes. *J Sol Energy Eng Trans ASME* 128(2):245–250
4. Chong K, Wong C (2009) General formula for on-axis sun-tracking system and its application in improving tracking accuracy of solar collector. *Sol Energy* 83(3):298–305
5. Jazar RN (2010) *Theory of applied robotics: kinematics, dynamics, and control*. Springer, New York
6. Jazar RN (2011) *Advanced dynamics: rigid body, multibody and aerospace applications*. Wiley, Hoboken
7. Legnani G, Casolo F, Righettini P, Zappa B (1996) A homogeneous matrix approach to 3D kinematics and dynamics I. *Mech Mach Theory* 31(5):573–587
8. Lever J, Ray L (2008) Revised solar-power budget for cool robot polar science campaigns. *Cold Regions Sci Technol* 52(2):177–190
9. Parkin RE (2010) Solar angles revisited using a general vector approach. *Sol Energy* 84(6):912–916
10. Randall J (2005) *Designing indoor solar products: photovoltaic technologies for AES*. Wiley, Hoboken
11. Rapp-Arraras I, Domingo-Santos JM (2009) Algorithm for the calculation of the horizontal coordinates of the sun via spatial rotation matrices. *Renew Energy* 34(3):876–882
12. Sansoni P, Francini F, Fontani D, Mercatelli L, Jafrancesco D (2008) Indoor illumination by solar light collectors. *Light Res Technol* 40(4):323–332
13. Sproul AB (2007) Derivation of the solar geometric relationships using vector analysis. *Renew Energy* 32(7):1187–1205

Nonlinear Approaches in Engineering Applications 2

Jazar, R.N.; Dai, L. (Eds.)

2014, XII, 317 p. 244 illus., 146 illus. in color.,

Hardcover

ISBN: 978-1-4614-6876-9